

Supporting information for

Photoelectrochemical Behavior of a Molecular Ru-Based Water-Oxidation Catalyst Bound to TiO₂-Protected Si Photoanodes

Roc Matheu,^{1,2} Ivan A. Moreno-Hernandez,³ Xavier Sala,⁴ Harry B. Gray,^{3,5} Bruce S. Brunschwig,³ Antoni Llobet,^{*1,4} Nathan S. Lewis^{*3,5,6}

¹Institute of Chemical Research of Catalonia (ICIQ), Avinguda Països Catalans 16, 43007 Tarragona, Spain.

²Departament de Química Física i Inorgànica, Universitat Rovira i Virgili, Marcel·lí Domingo s/n, 43007 Tarragona, Spain.

³ Division of Chemistry and Chemical Engineering, California Institute of Technology, Pasadena, CA 91125, USA

⁴Departament de Química, Universitat Autònoma de Barcelona, Cerdanyola del Vallès, 08193 Barcelona, Spain

⁵ Beckman Institute, California Institute of Technology, Pasadena, CA 91125, USA

⁶ Kavli Nanoscience Institute, California Institute of Technology, Pasadena, CA 91125, USA.

OUTLINE

Outline	S2
1.Materials and Methods	S3
1.1 General Materials	S3
1.2 General Methods	S3
1.3 Preparation of Si/TiO ₂ /C substrates	S3
1.4 Preparation of Si/TiO ₂ /C/CNT substrates	S3
1.5 Preparation of Si/TiO ₂ /C/CNT/ 1 substrates	S4
1.6 Preparation of electrodes	S4
1.7 Preparation of Si/TiO ₂ /C/CNT/[1+1(O)] electrodes	S4
1.8 Preparation of Phosphate solutions	S4
1.9 Photoelectrochemical Methods	S5
Average loading and current density of electrodes	S8
Picture of hole pattern	S9
SEM analysis of Si/TiO ₂ /C/CNT/[1+1(O)] substrates	S10
EDX analysis of Si/TiO ₂ /C/CNT/ 1 substrates	S11
Fe(CN) ₆ ³⁻ /Fe(CN) ₆ ⁴⁻ Measurements	S12
Electrochemical data at pH = 7 of Si/TiO ₂ /C and Si/TiO ₂ /C/CNT electrodes	S13
Example of coverage estimation	S14
Faradaic efficiency determination	S14
Cyclic voltammetry of Si/TiO ₂ /C/CNT/[1+1(O)] before and after 1 h of oxygen evolution	S15
Chronopotentiometry and CV experiments for 3 h of oxygen evolution	S16
References	S17

1. MATERIALS & METHODS

1.1 General Materials

Na_2HPO_4 , NaH_2PO_4 , $\text{K}_3\text{Fe}(\text{CN})_6$, $\text{K}_4\text{Fe}(\text{CN})_6 \cdot 3\text{H}_2\text{O}$, NH_4OH , HCl , poly(methyl methacrylate) (PMMA), tetrakis-dimethylamidotitanium (99.999%) (Sigma-Aldrich), anhydrous methanol (99.8%, Sigma-Aldrich), tetrahydrofuran (99.9 %, inhibitor free, Sigma Aldrich) and buffered HF (Transene Company, Inc.) were used as received. Silicon wafers (Addison Engineering, Inc.), multiwalled C nanotubes (D.D > 50 nm) (HeJi, Inc), In–Ga eutectic alloy (99.99%) (Alfa-Aesar), and Ag Paint (SPI, INC) were purchased from commercial suppliers. The pyrolytic graphite target, 99.999% pure C, was acquired from ACI Alloys and was used as a C target for sputtering. The $\text{Ru}(\text{tda})(\text{py-pyr})_2$ complex was synthesized as reported previously.¹

1.2 General methods

A Fuji F200 Ultratech was used for atomic-layer deposition (ALD) and an AJA Orion was used for sputtering. An environmental scanning-electron microscope from FEI (Quanta 600) with an energy-dispersive X-ray (EDX) detector (Oxford Instruments) was used for EDX and SEM measurements, and an EPSON Perfection v39 was used as an optical scanner. The pH of the solutions was determined by a pH meter (CRISON, Basic 20+) that was calibrated before measurements by use of standard solutions at pH= 4.01, 7.00 or 9.21. Oxygen evolution was analyzed with a gas-phase Clark-type oxygen electrode (Unisense Ox-N needle microsensor) that was calibrated by addition of small quantities of $\text{O}_2(\text{g})$ (99%). A Dektak XT stylus was used for profilometry.

1.3 Preparation of Si/TiO₂/C substrates

The preparation was adapted from the literature.² n-Si(100) wafers (P-doped with a resistivity $\rho = 0.1\text{--}0.3\ \Omega\cdot\text{cm}$, $525 \pm 25\ \mu\text{m}$ thick) or p⁺-Si(100) wafers (B-doped with $\rho < 0.005\ \Omega\cdot\text{cm}$, $381 \pm 25\ \mu\text{m}$ thick) were cleaned using an RCA etch process that consisted of (1) etching the wafer with buffered HF(aq); (2) soaking the wafer in a 5:1:1 (by volume) $\text{H}_2\text{O}/\text{H}_2\text{O}_2/\text{NH}_4\text{OH}$ solution at 75 °C for 10 min; (3) etching the wafers again with buffered HF(aq); and then (4) soaking the wafers in a 5:1:1 $\text{H}_2\text{O}/\text{H}_2\text{O}_2/\text{HCl}$ solution at 75 °C for 10 min. TiO₂ was deposited on the films by ALD using tetrakis-dimethylamidotitanium (TDMAT) and H₂O as reagents. Each ALD cycle consisted of a 0.060 s pulse of distilled, deionized H₂O (18.2 M $\Omega\cdot\text{cm}$ resistivity, Millipore) followed by a 0.25 s TDMAT pulse. After each pulse, N₂(g) was purged through the chamber for 15 s at a flow rate of 20 sccm. A total of 1250 cycles were performed. The substrate was maintained at 150 °C during the deposition, and the TDMAT precursor was heated to 75 °C with a heating jacket. The H₂O was maintained at room temperature. C was sputtered using a pyrolytic graphite target in an Ar plasma. A RF power source of 150 W was maintained for 2 h and the gas flow rate was 20 psi of Ar at a total pressure of 5 mTorr. No intentional heating was provided to the samples during deposition. The thickness of the layer was determined by profilometry.

The Si/TiO₂ electrode as-prepared is not conductive due the resistance of the top-most TiO₂ layer.² Consequently, the molecular catalysts was not deposited directly on Si/TiO₂ substrates as was done on electrodes with conductive TiO₂/SnO₂ layers.^{3,4} The layer of sputtered C makes

the electrodes conductive, while the pyrene pi-stacking provided the anchor for the molecular catalysts on the drop-casted CNT materials.

1.4 Preparation of Si/TiO₂/C/CNT substrates

The Si/TiO₂/C substrates were cleaved into pieces $\sim 0.25 \text{ cm}^2$ in area, with the actual area measured using an optical scanner and ImageJ software. A suspension of multiwalled carbon nanotubes (CNT) was prepared by sonicating the CNT for 1 h in tetrahydrofuran (THF) (1 mg / 1 mL). $600 \mu\text{L cm}^{-2}$ of the suspension was then deposited on the Si/TiO₂/C substrates, using several volumes (10 times $60 \mu\text{L cm}^{-2}$) with the use of an Eppendorf pipette, to avoid overflow. The samples were air-dried for 10 min and $60 \mu\text{L cm}^{-2}$ of a PMMA solution in dichloromethane (0.25 mg mL^{-1}) was added onto the electrodes. This process resulted in a nominal coverage of 0.6 mg cm^{-2} of CNT. The samples were dried for 2 h at room temperature. Holes were carefully scratched on top of the Si/TiO₂/C/CNT substrates using a $0.64 \pm 0.01 \text{ mm}$ diameter mask with a pitch of $1.02 \pm 0.05 \text{ mm}$ (Figure S1) and a pointer of $\sim 0.2 \text{ mm}$ diameter. The surface area of the CNT is $40\text{--}600 \text{ cm}^2 \text{ mg}^{-1}$, as calculated from the ratio of the surface area of the CNT to the geometric area of $24\text{--}360$.⁵ This value is in good agreement with the ratio estimated from electrochemical measurements described in more detail below.

1.5 Preparation of Si/TiO₂/C/CNT/1 substrate

Si/TiO₂/C/CNT substrates were soaked in a solution of complex **1** in methanol (0.30 mM) for 12 h, rinsed with a fresh solution of methanol, air-dried, and analyzed by EDX and electrochemical techniques. The EDX of the modified electrodes clearly showed the incorporation of the Ru on the substrates (Figure S3).

1.6 Preparation of Si/TiO₂/C, Si/TiO₂/C/CNT and Si/TiO₂/C/CNT/1 electrodes

The preparation of electrodes based on Si/TiO₂/C, Si/TiO₂/C/CNT and Si/TiO₂/C/CNT/1 substrates was adapted from the literature.² In–Ga eutectic alloy was used to scribe the back side of the samples to make an Ohmic contact. A Sn-coated Cu wire was passed through a glass tube and affixed to the In–Ga by Ag paint. Once the Ag paint had dried, epoxy was used to seal the samples to the glass tube. The resulting exposed active area of each electrode was measured with an optical scanner and ImageJ software. The area of the final samples was between $0.1 \text{ cm}^2\text{--}0.2 \text{ cm}^2$.

1.7 Preparation of Si/TiO₂/C/CNT/[1+1(O)] electrodes

Electrodes of Si/TiO₂/C/CNT/1 were used as working electrodes in a pH = 12 phosphate solution in which a Pt wire and Hg/Hg₂SO₄ were used as counter and reference electrodes, respectively. A potential of 1.30 vs NHE was applied to the p⁺-Si/TiO₂/C/CNT/1 electrodes in the absence of illumination whereas a potential of 1.10 V vs NHE was applied to the n-Si/TiO₂/C/CNT/1 electrodes under 3 Sun illumination. The electrodes were then rinsed with fresh water and dried in air.

Analogous systems have been studied in solution and immobilized on glassy carbon electrodes.^{1,6} In both cases, the amount of Ru=O generated in situ was not sufficient for extended catalysis and thus more time at oxidizing potentials was required to produce sufficient Ru=O, as was done in the present work. Molecular Ru catalysts that form RuO₂ upon decomposition show enhanced performance.⁷ Extremely positive potentials were avoided in this work to minimize such effects.

1.8 Preparation of Phosphate solutions

pH = 7.0 buffered solution (I = 0.1 M): powders of NaH₂PO₄ (2.31 g, 0.0193 M) and Na₂HPO₄ (3.77g, 0.0266 M) were dissolved with sufficient deionized H₂O to make up 1 L of solution.

pH = 12.0 buffered solution (I = 0.1 M): powders of Na₂HPO₄ (10.293g, 0.0073 M) and Na₃PO₄ (2.06g, 0.0126 M) were dissolved with sufficient deionized H₂O to make up 1 L of solution.

1.9 Photoelectrochemical Methods

1.9.1 Instruments

A Bio-Logic model SP-200 potentiostat or a CH Instruments CHI660d potentiostat were used in a 3-electrode configuration.

1.9.2 Fe(CN)₆³⁻/Fe(CN)₆⁴⁻, pH = 7 and pH = 12 measurements

Techniques

Cyclic voltammetry (CV) was performed at 40 mV s⁻¹ unless otherwise specified. Chronoamperometry for 150 s was used for the generation of **1(O)** by applying a potential of 1.05 V to n-Si electrodes and 1.30 V to p⁺-Si electrodes.

The surface roughness of Si/TiO₂/C/CNT electrodes was estimating using the capacitance of the electrode obtained from the CV (Figure S5) made using the CHI660d potentiostat. The CHI660d digital potentiostat reports the average current at each potential step by taking the mean of 500 current measurements made on the step. This current is equivalent to the current that an analog potentiostat measures. The figure shows a difference between the cathodic and anodic scans of ~0.2 mA cm⁻² at a scan rate of 40 mV s⁻². This difference yields a nominal capacitance of ~2 mF cm⁻² based on the geometric area of the electrode. A specific capacitance of ~0.04 mF cm⁻² is observed based on the electrochemically active area.⁸ These values allow estimation of an approximate ratio of 50 between the electrochemically active surface area and the geometric area of the electrode.

Chronopotentiometry was performed at 1 mA cm⁻². For all measurements at pH = 7, the electrochemical data were corrected for uncompensated resistance (90 % corrected).

Chronopotentiometry (CP) was used to evaluate the OER electrode stability.⁸ The CP technique fixed the current density at 1 mA cm⁻². The potentials observed in the CVs at 1 mA cm⁻² (p⁺, 1.33 V; 1 sun, 1.28 V; 2 sun, 1.18 V; and 3 sun: 1.08 V) are slightly lower than those observed after 0.05 h in the CP experiment (p⁺, 1.34 V; 1 sun, 1.38 V; 2 sun, 1.20 V; and 3 sun: 1.08 V) due to the contribution of the anodic non-faradaic current in the CV (0.1 mA·cm⁻²) not present in the CP technique. However, these observations are limited by the experimental variability among the samples (Table S1 and S2)

Electrodes

An n-Si/TiO₂/C/CNT/[1+1(O)] sample or p⁺-Si/TiO₂/C/CNT/[1+1(O)] sample was used as a working electrode. For measurements in contact with Fe(CN)₆³⁻/Fe^{II}(CN)₆⁴⁻(aq), two distinct Pt disks were used as the counter and reference electrodes, respectively. For measurements at pH =7 and at pH = 12, a Pt wire was used as a counter electrode and Hg/Hg₂S₂O₄ was used as a reference electrode. The Pt wire was separated from the solution by a membrane (Sintered Glass Filter Discs, Porosity D, aceglass®)

Cells

A 100 mL home-made cell consisted of 5 openings at the top into which the working, counter and reference electrodes were placed, with the cell also containing a 12 x 3 mm stir bar.

Solutions

A phosphate buffered solution was used for measurements at pH= 7 and at pH = 12. For measurements in contact with Fe(CN)₆³⁻/Fe^{II}(CN)₆⁴⁻, a solution containing 350 mM of Fe(CN)₆³⁻, 50 mM K⁺/Fe^{II}(CN)₆⁴⁻ and 1.0 M KCl(aq) was used.

1.9.3 Light source and calibration

Illumination during cyclic voltammetry and other measurements under light was provided by a Xe lamp (300 W, USHIO) with a quartz filter (cut off at 400 nm). Before addition of solution to the cell, a calibrated silicon photodiode was used to adjust the light intensity of the solar illuminator on the working electrode to the same reading that would be observed under AM 1.5G of solar radiation with a total light intensity of 100 mW/cm², 1 Sun. The distance of the solar illuminator from the cell could be adjusted to achieve an intensity of 1, 2 or 3 Sun of simulated AM 1.5G light.

1.9.4 O₂ Evolution

Bulk electrolysis was performed using a 10 mL two-compartment cell with a sintered glass filter disc (aceglass®, Porosity D) separator between the two compartments. Both compartments were filled with 5 mL of pH = 7 solution and both compartments were equipped with a stir bar. A Ag/AgCl (KCl sat.) electrode was used as the reference. The counter electrode was placed in one compartment and the working electrode, reference

electrode and a Clark electrode to measure oxygen evolution and to calculate the Faradaic efficiency, were in the other compartment. At the end of the bulk electrolysis, the Clark electrode was calibrated by addition of known volumes of 99% purified O₂(g).

1.9.5 Surface coverage Estimation (Γ)

The surface coverage (Γ) of complexes **1** and **1(O)** on the electrodes was estimated by applying the formula $\Gamma \text{ (mol}\cdot\text{cm}^{-2}\text{)} = Q / (n \cdot S \cdot F)$, where Q is the charge under the Ru^{III}/Ru^{II} cathodic wave of the **1** and **1(O)** species, n is the number of electrons involved in the electron transfer (1 e⁻ in all the cases), S is the geometric surface area of the electrode, and F is Faraday's constant. The integration of the cathodic wave for the two species requires the use of a baseline for each peak. The drawing of an accurate baseline is difficult, particularly for the **1(O)** peak, because the two peaks are close together (Figure S6). The ratio for the concentrations of **1** and **1(O)** was calculated by dividing the Γ of the former by the Γ of the latter. Figure S6 provides an example of the estimation of the coverage, whereas Table S1 contains the resulting coverage values.

The average coverage was estimated from 5 independent experiments and the standard deviation between samples was used to estimate the standard error; however, the actual error maybe substantially larger due to systematic error in drawing the baseline. For individual experiments, the value for the coverage of the sample is provided in the captions of the related figures.

1.9.6 Attempts to analyze the samples by XPS and ICP-MS/OES

The XPS C 1s and the Ru 3d_{3/2}, Ru 3d_{5/2} signals overlap because of the high content of C relative to Ru and the close proximity of the binding energies. The overlap prevented detection of RuO₂. ICP-MS/OES was not performed because a submonolayer of Ru is expected to yield a concentration of Ru in solution that is below the detection limit of the technique.

Table S1: Loading of the molecular complexes **1** and **1(O)** on n-Si/TiO₂/C/CNT/**1**, n-Si/TiO₂/C/CNT/[**1+1(O)**], p⁺-Si/TiO₂/C/CNT/**1** and p⁺-Si/TiO₂/C/CNT/[**1+1(O)**] electrodes.

	Γ_1 (nmol cm ⁻²) on Si/TiO ₂ /C/CNT/ 1	$\Gamma_1 / \Gamma_{1(O)}$ (nmol cm ⁻²) on Si/TiO ₂ /C/CNT/[1+1(O)]
p⁺-Si	14.6 ± 2.4	3.0 ± 0.8 / 1.2 ± 0.6 (ratio $_{1/1(O)}$ = 2.5 ± 1.0)
n-Si	13.0 ± 2.2	2.9 ± 0.8 / 0.7 ± 0.3 (ratio $_{1/1(O)}$ = 4.2 ± 1.3)

Table S2: Current density (*J*, mA cm⁻²) measured at 1.30 V for n-Si/TiO₂/C/CNT/[**1+1(O)**] electrodes at pH = 7 at different light intensities.

1 Sun	2 Sun	3 Sun
<i>J</i> = 0.9 ± 0.1 mA cm ⁻²	<i>J</i> = 1.4 ± 0.1 mA cm ⁻²	<i>J</i> = 1.8 ± 0.2 mA cm ⁻²

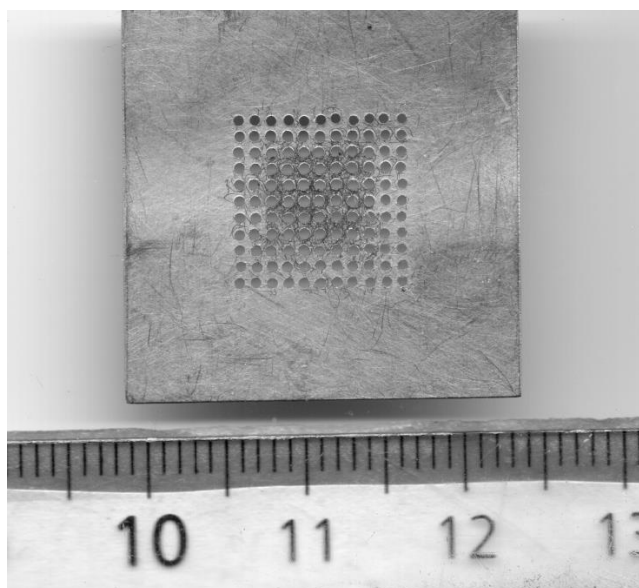


Figure S1: Aluminum foil with patterned $0.32 \pm 0.01 \text{ mm}^2$ holes (diameter = $0.64 \pm 0.01 \text{ mm}$) with a pitch of $1.02 \pm 0.05 \text{ mm}$ that was used to prepare Si/TiO₂/C/CNT electrodes. A cm ruler is shown for comparison.

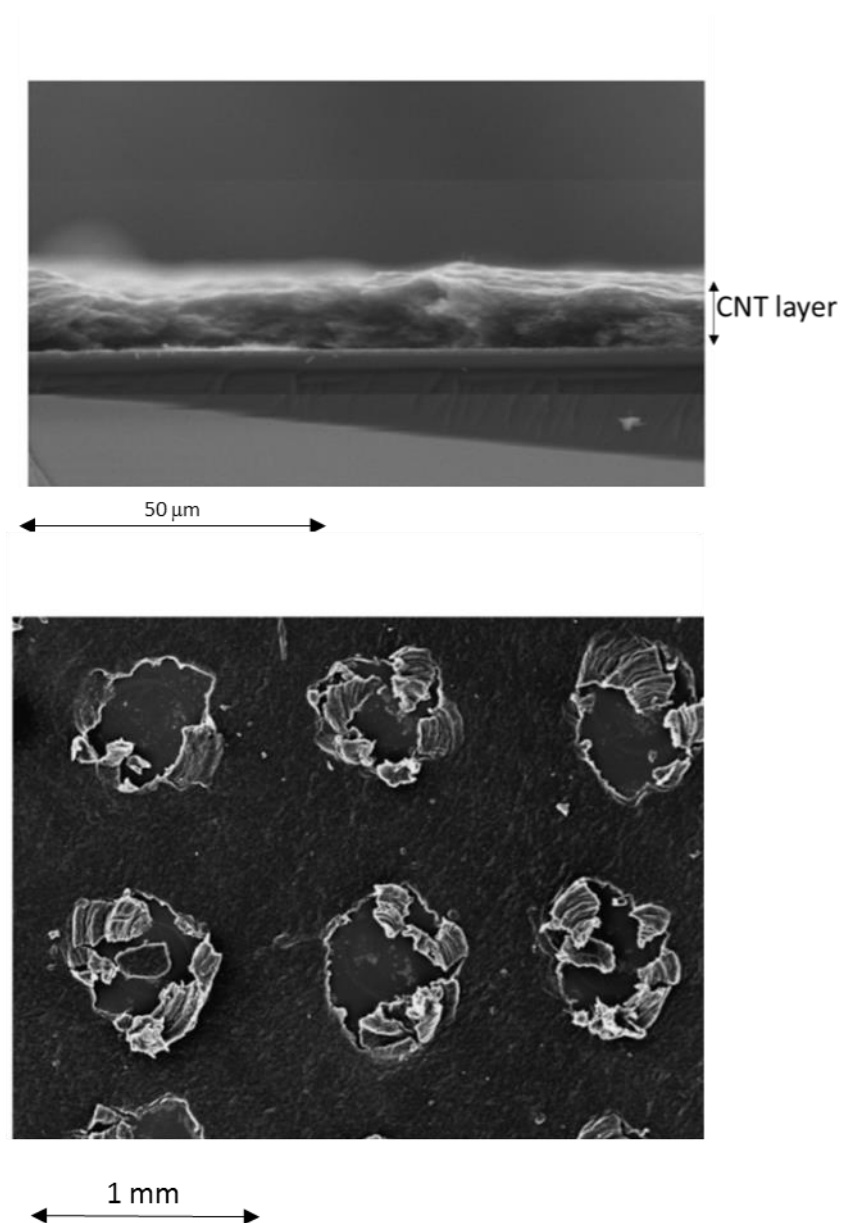


Figure S2: Representative SEMs of Si/TiO₂/C/CNT/1 electrodes: Top, cross-section showing the $14 \pm 1 \mu\text{m}$ thick layer of CNT; Bottom, front view of Si/TiO₂/C/CNT/1 showing the $0.21 \pm 0.01 \text{ mm}^2$ holes (diameter = $0.52 \pm 0.02 \text{ mm}$) separated by $1.10 \pm 0.06 \text{ mm}$. The measured size of the holes lead to an estimated 18% of area of the Si/TiO₂/C/CNT/1 substrates exposed to the illumination.

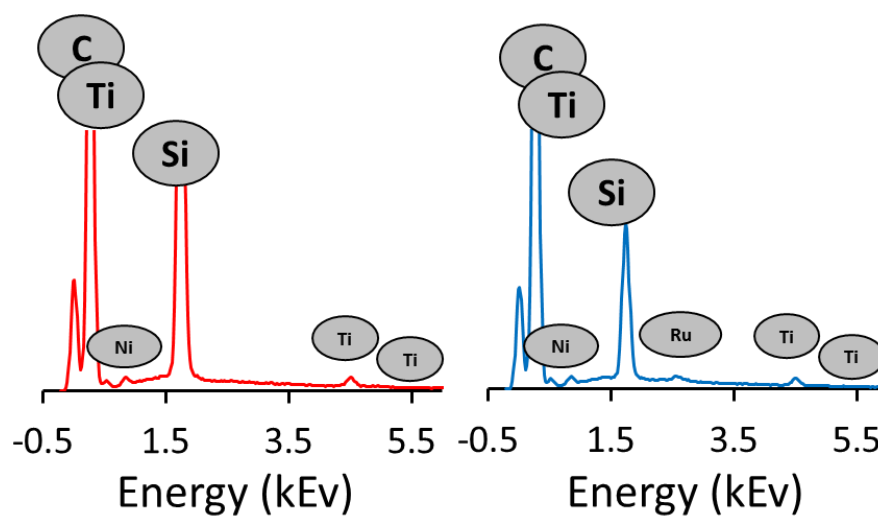


Figure S3: EDX profiles of a Si/TiO₂/C/CNT sample before (left) and after (right) soaking in a solution that contained **1**: left, EDX spectra of substrates after soaking (Si/TiO₂/C/CNT); and right EDX spectra of Si/TiO₂/C/CNT/**1**. The measured amount in the Si/TiO₂/C/CNT/**1** substrate was 0.8 % by weight. The traces of Ni content in the CNT are due to the synthesis as indicated by the CNT supplier.⁵

Fe(CN)₆³⁻/Fe(CN)₆⁴⁻ Measurements

The electrical properties of the p⁺-Si electrodes without an attached catalyst were analyzed by measuring the current density vs potential (*J* - *E*) response in a 350 mM [Fe(CN)₆]³⁻ - 50 mM [Fe(CN)₆]⁴⁻ (aq) solution (Figure S4). The p⁺-Si/TiO₂/C electrodes exhibited small (~60 mV) kinetic overpotential at anodic current densities of 10 mA cm⁻², in accord with previous reports for p⁺-Si/TiO₂ electrodes.² The overpotential of the p⁺-Si/TiO₂/C/CNT electrodes (~30 mV) was less than that of p⁺-Si/TiO₂/C electrodes, presumably due to the roughness of the CNT layer. Figure S5 shows the CVs for the n-Si electrode with and without the CNT layer at pH = 7.0. The capacitive charging currents were much larger for the electrodes with the CNT layer, being ~0.2 mA cm⁻² at a scan rate of 40 mV s⁻¹, suggesting a 50-fold increase in the electrochemically active surface area of the electrode. The electrochemical response of the electrodes was identical with or without the PMMA, confirming the electrochemical inertness of the PMMA under the test conditions and indicating that the PMMA layer did not block solution contact with the electrode.

For n-type electrodes, measurements under illumination allowed estimation of the photovoltage (*V*_{oc}) and the photogenerated current density (*J*_{*l*}). Under simulated 1 Sun illumination, the n-Si/TiO₂/C electrode showed *V*_{oc} = -295 ± 20 mV and *J*_{*l*} = 10.7 ± 1.7 mA cm⁻², similar to related photoanodes in 350 mM [Fe(CN)₆]³⁻ - 50 mM [Fe(CN)₆]⁴⁻ - 1.0 M KCl(aq) (Figure S4B).^{2,9} The n-Si/TiO₂/C/CNT electrodes with no holes exhibited virtually no light-induced current density (*J* = 0.08 ± 0.01 mA cm⁻²), whereas with holes present, the value of *J*_{*l*} = 2.0 ± 0.3 mA cm⁻² was consistent with the 18% of exposed area arising from the hole patterning step.

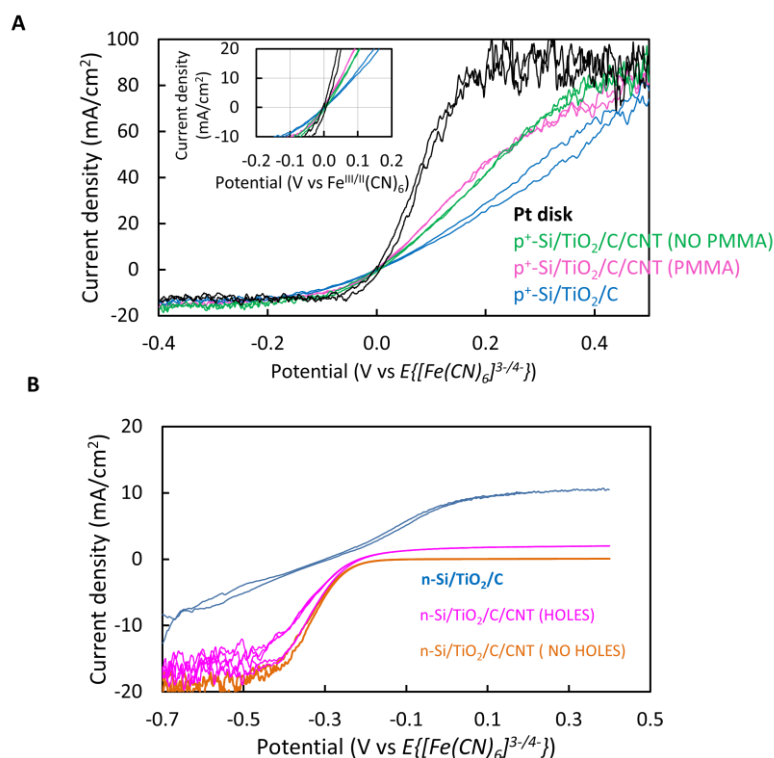


Figure S4. Determination of the photoelectrochemical properties of p⁺ and n-Si/TiO₂/C/CNT electrodes by electrochemical measurements in Fe(CN)₆^{3-/4-} (aq). **A** Cyclic voltammetry for p⁺-Si/TiO₂/C electrodes in Fe(CN)₆^{3-/4-} (350 mM, 50 mM, 1.0 M KCl(aq), scan rate 40 mV s⁻¹) compared to a Pt disk (dark line). Inset: Expansion of the -10 mA cm⁻² to 10 mA cm⁻² current

density region. Relative to the Pt disk, at 10 mA cm^{-2} on $\text{p}^+\text{-Si/TiO}_2/\text{C}$ (blue solid line) and $\text{p}^+\text{-Si/TiO}_2/\text{C/CNT}$ (pink solid line) electrodes, the potential loss was $\sim 60 \text{ mV}$ and 30 mV , respectively. The electrochemical response of $\text{p}^+\text{-Si/TiO}_2/\text{C/CNT}$ was essentially identical with and without a PMMA layer (pink and green lines respectively). **B** Representative cyclic voltammetry for n-Si electrodes in a $\text{Fe(CN)}_6^{3-/4-}$ solution (350 mM , 50 mM , 1.0 M KCl(aq)) under 1 Sun illumination. The V_{oc} and the light-limited current density (J_{l}) were estimated from the average behavior of 3 independent electrodes: $\text{Si/TiO}_2/\text{C}$, blue solid line, $V_{\text{oc}} = -295 \pm 20 \text{ mV}$, $J_{\text{l}} = 10.7 \pm 1.7 \text{ mA cm}^{-2}$; $\text{Si/TiO}_2/\text{C/CNT}$, pink solid line, $V_{\text{oc}} = -220 \pm 20 \text{ mV}$, $J_{\text{l}} = 2.0 \pm 0.3 \text{ mA cm}^{-2}$; and $\text{Si/TiO}_2/\text{C/CNT}$ without holes, orange solid line, $V_{\text{oc}} = -70 \pm 30 \text{ mV}$, $J_{\text{l}} = 0.08 \pm 0.01 \text{ mA cm}^{-2}$.

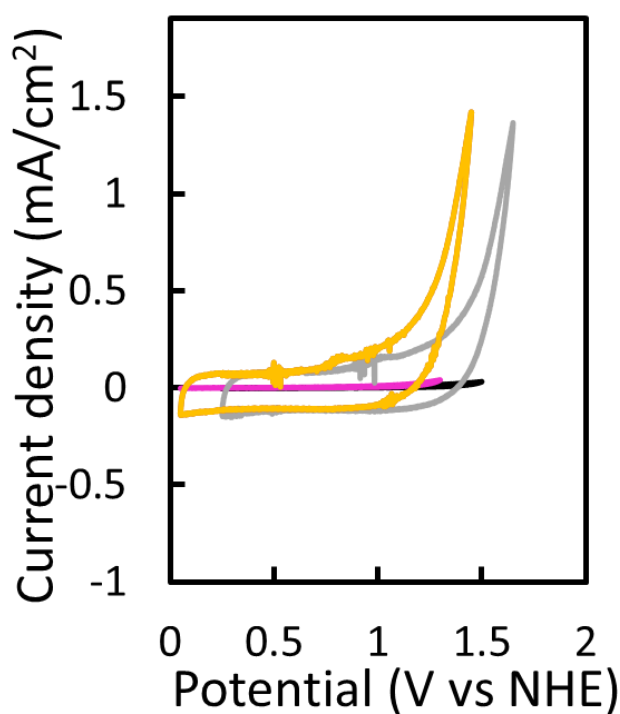


Figure S5. Cyclic voltammetry of bare n-Si/TiO₂/C/CNT (yellow line) and n-Si/TiO₂/C electrodes (pink line) under 3 Sun illumination at pH = 7 together with CVs of p⁺-Si/TiO₂/C/CNT (grey line) and p⁺-Si/TiO₂/C (black line) electrodes in the dark at pH = 7. All scans at 40 mV s^{-1} .

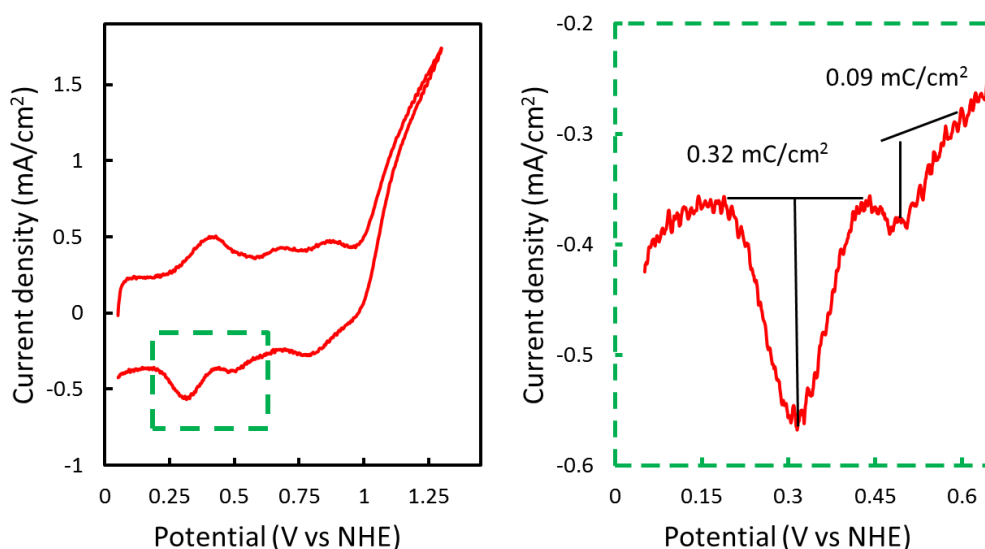


Figure S6: Cyclic voltammetry of n-Si/TiO₂/C/CNT/[1+1(O)] ($\Gamma_1 = 3.25 \text{ nmol cm}^{-2}$, $\Gamma_{1(0)} = 0.9 \text{ nmol cm}^{-2}$, ratio $1/1(0) = 3.3$) under 3 Sun illumination at pH = 7 (red line, left) together with a representation of the integration of the III/II cathodic waves of **1** and **1(O)** species, to determine the surface coverage (right). The scan rate was 40 mV s^{-1} .

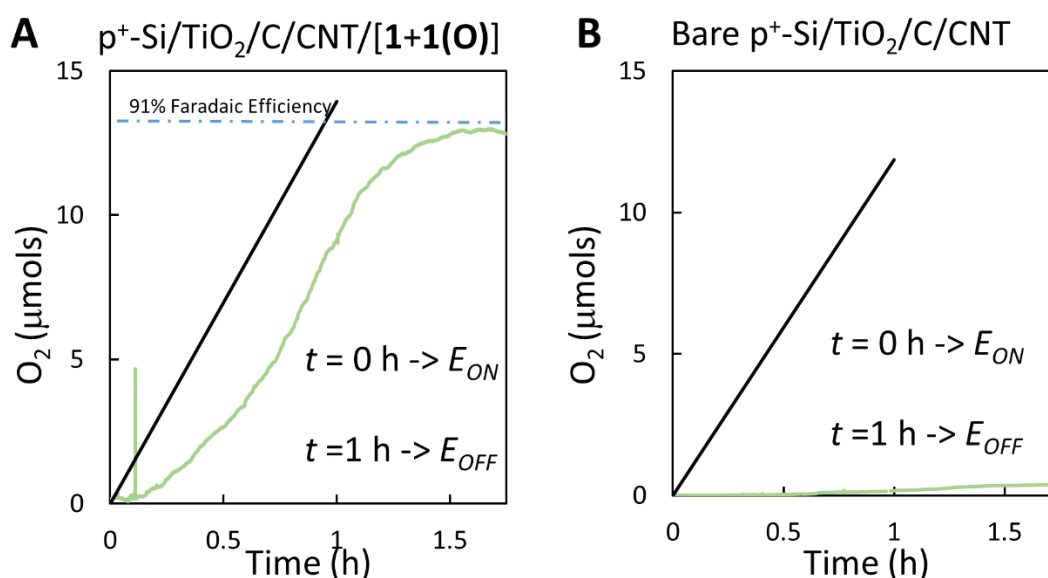


Figure S7. Representative plot for measured O₂ evolution (green solid lines) and theoretical O₂ evolution (black solid line) against time for **A**, a p⁺-Si/TiO₂/C/CNT/[1+1(O)] electrode ($\Gamma_1 = 2.7 \text{ nmol cm}^{-2}$, $\Gamma_{1(0)} = 1.0 \text{ nmol cm}^{-2}$, ratio **1/1(0)** = 2.7, $S = 1.5 \text{ cm}^2$), and **B**, a bare p⁺-Si/TiO₂/C/CNT electrode ($S = 1.4 \text{ cm}^2$). The oxygen evolution was a result of a chronopotentiometry at $J = 1 \text{ mA cm}^{-2}$ and the theoretical oxygen evolution (nO_2) was calculated applying the formula $nO_2 = Q/(4 \cdot F)$, where Q is the charge passed during the experiment and F is Faraday's constant. The sigmoidal response of the O₂ evolution was a result of the large number of bubbles accumulated at the surface of the electrodes.^{1,7}

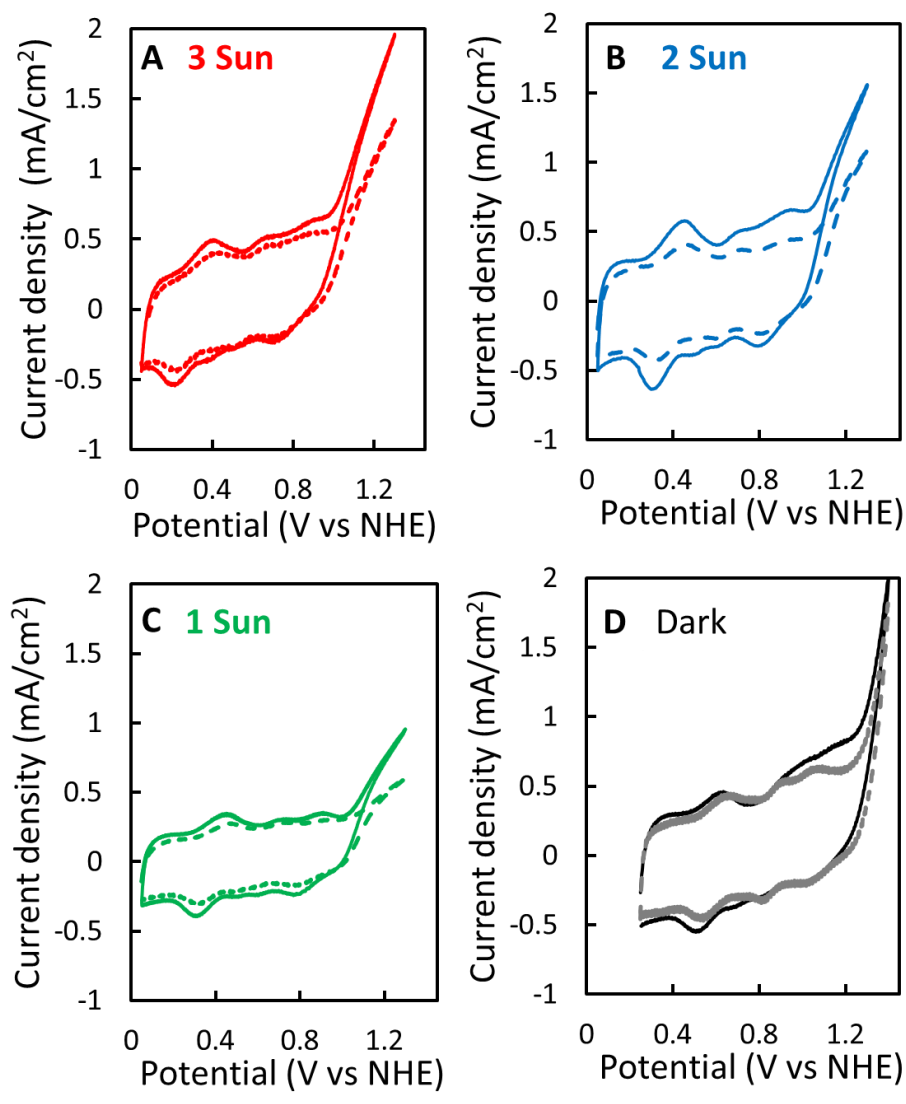


Figure S8: Cyclic voltammetries before (solid lines) and after (dashed line) a Chronopotentiometric experiment at $J = 1 \text{ mA cm}^{-2}$ at $\text{pH} = 7$ at a scan rate of 40 mV s^{-1} : **A**, n-Si/TiO₂/CNT/C/[1+1(O)] under 3 Sun illumination ($\Gamma_1 = 3.62 \text{ nmol cm}^{-2}$, $\Gamma_{1(0)} = 0.9 \text{ nmol cm}^{-2}$, ratio $_{1/1(0)} = 3.9$); **B**, n-Si/TiO₂/CNT/C/[1+1(O)] under 2 Sun illumination ($\Gamma_1 = 3.3 \text{ nmol cm}^{-2}$, $\Gamma_{1(0)} = 0.9 \text{ nmol cm}^{-2}$, ratio $_{1/1(0)} = 3.5$); **C**, n-Si/TiO₂/CNT/C/[1+1(O)] under 1 Sun illumination ($\Gamma_1 = 2.7 \text{ nmol cm}^{-2}$, $\Gamma_{1(0)} = 0.8 \text{ nmol cm}^{-2}$, ratio $_{1/1(0)} = 3.5$); and **D**, p⁺-Si/TiO₂/CNT/C/[1+1(O)] in dark conditions ($\Gamma_1 = 2.9 \text{ nmol cm}^{-2}$, $\Gamma_{1(0)} = 2.5 \text{ nmol cm}^{-2}$, ratio $_{1/1(0)} = 2.5$). See Figure 2 in the main section for the chronopotentiometry data.

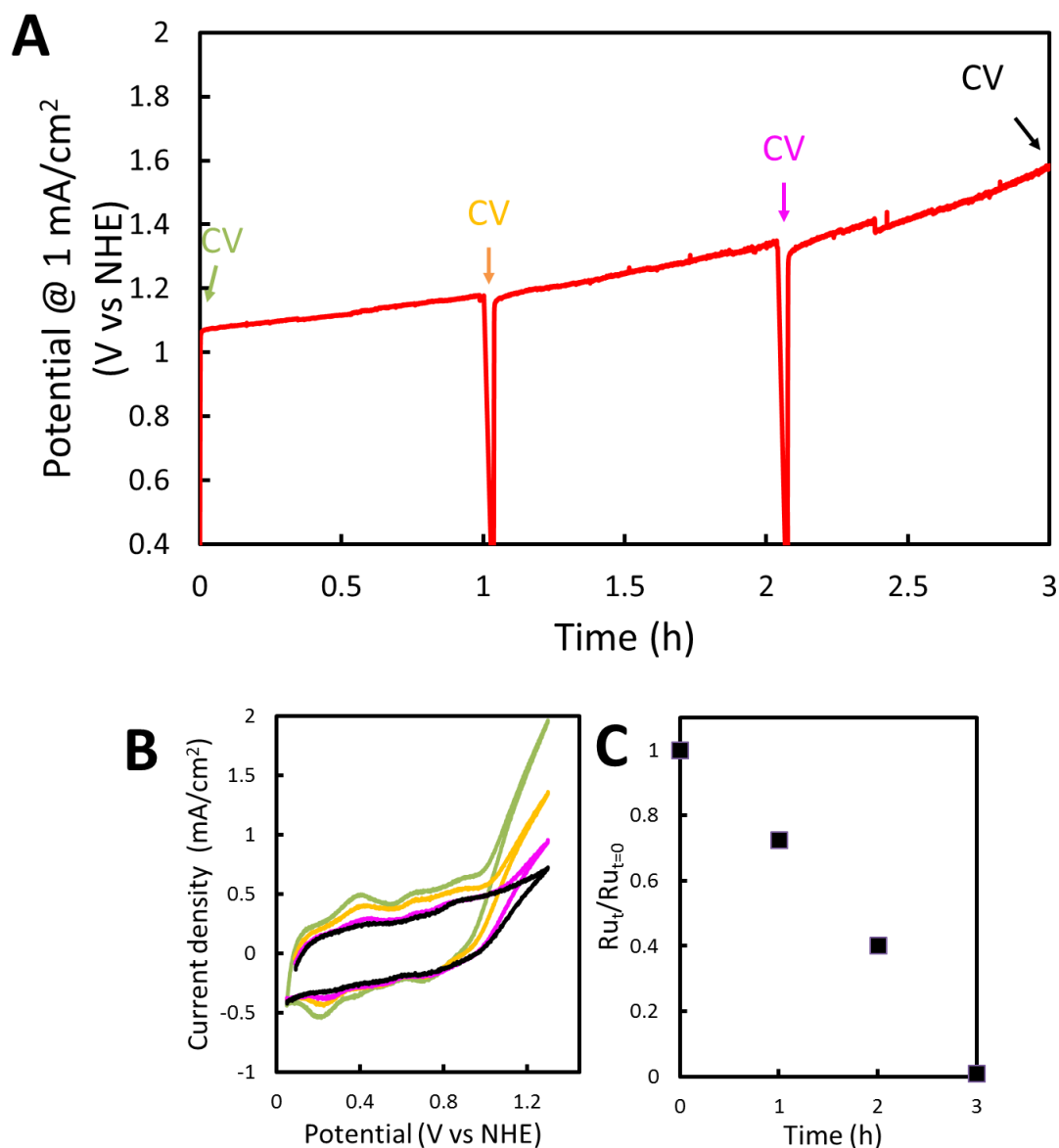


Figure S9: **A**, Chronopotentiometry (at $J = 1 \text{ mA cm}^{-2}$) for n-Si/TiO₂/C/CNT/[1+1(O)] ($\Gamma_1 = 3.62 \text{ nmol cm}^{-2}$, $\Gamma_{1(0)} = 0.9 \text{ nmol cm}^{-2}$, ratio $_{1/1(0)} = 3.9$) under 3 Sun illumination at pH = 7. **B**, CVs of the electrodes were performed at $t = 0, 1, 2$ and 3 h . **C**, Normalized quantification of the loss of $\text{Ru}_t/\text{Ru}_{t=0}$ against time (t). $\text{Ru}_t/\text{Ru}_{t=0}$ was estimated from the charge of the cathodic portion of the III/II wave of complex **1**. Tables S3 and S4 provide the estimated turnover numbers obtained from analysis of these data.

Table S3: Estimation of turnover number (TON) assuming that **1(O)** is responsible for all of the catalytic O₂ evolution in the three-hour chronopotentiometry (Figure S9).

	nmols 1(O)	nmols O ₂	TONS
0 h < t < 1 h	0.142	1436	10 112
1 h < t < 2 h	0.099	1436	14 500
2 h < t < 3 h	0.035	1436	40 000
Total			~ 60 000

Table S4: Estimation of turnover number (TON) assuming that **[1+1(O)]** is responsible for all of the catalytic O₂ evolution in the three-hour chronopotentiometry (Figure S9).

	nmols [1+1(O)]	nmols O ₂	TONS
0 h < t < 1 h	0.700	1436	2 051
1 h < t < 2 h	0.488	1436	2 942
2 h < t < 3 h	0.175	1436	8 205
Total			~ 13 000

REFERENCES

- ¹ Creus, J.; Matheu, R.; Peñafiel, I.; Moonshiram, D.; Blondeau, P.; Benet-Buchholz, J.; García-Antón, J.; Sala, X.; Godard, C.; Llobet, A. *Angew. Chem. Inter. Ed.* **2016**, *55*, 15382-15386.
- ² Hu, S.; Shaner, M. R.; Beardslee, J. A.; Lichterman, M.; Brunschwig, B. S.; Lewis, N. S. *Science* **2014**, *344*, 1005-1009.
- ³ Sheridan, M. V.; Sherman, B. D.; Coppo, R. L.; Wang, D.; Marquard, S. L.; Wee, K.-R.; Murakami Iha, N. Y.; Meyer, T. J. *ACS Energy Lett.* **2016**, *1*, 231-236
- ⁴ Sheridan, M. V.; Hill, D. J.; Sherman, B. D.; Wang, D.; Marquard, S. L.; Wee, K.-R.; Cahoon, J. F.; Meyer, T. J. *Nano Letters* **2017**, *17*, 2440-2446.
- ⁵ HeJi supplier, www.nanotubes.eu.com/nano/products/M4906/main.html
- ⁶ McCrory, C. C. L.; Jung, S.; Ferrer, I. M.; Chatman, S. M.; Peters, J. C.; Jaramillo, T. F. *J. Am. Chem. Soc.* **2015**, *137*, 4347-4357
- ⁷ Matheu, R.; Francàs, L.; Chervnev, P.; Ertem, M. Z.; Batista, V.; Haumann, M.; Sala, X.; Llobet, A. *ACS Catal.* **2015**, *5*, 3422-3429.
- ⁸ McCrory, C. C. L.; Jung, S.; Ferrer, I. M.; Chatman, S. M.; Peters, J. C.; and Jaramillo, T. F. *J. Am. Chem. Soc.* **2015**, *137*, 4347-4357.
- ⁹ The light intensity was calibrated before the [Fe(CN)₆]^{3-/4-} addition.